Iranian Journal of Basic Medical Sciences

ijbms.mums.ac.ir

Efficacy of finerenone and/or roflumilast in alleviation of intestinal ischemic reperfusion injury via regulation of IL10/AMPK/VEGF/eNOS pathway in rats

Marwa Monier Mahmoud Refaie [1, 2], Randa Ahmed Ibrahim [3, 2], Sayed Shehata [4], Asmaa A. Muhammed [5, 6], Shereen Mohammed Mohammed Elsaghir [7], Asmaa S.M. Abdel Fattah [7], Asmaa A. Hasan [8], Amany H. Abdel Naiem [9, 2*], Nagwa Zenhom Mustafa Ahmed [9, 10], Mohamed Rabie Saad [11], Doaa Mohamed Elroby Ali [12], Heba A. Habib [13], Nardien Ekram Haliem Saleh [14]

[1] Department of Medical Pharmacology, Faculty of Medicine, Minia University, 61511, Minia, Egypt
[2] Faculty of Medicine, Minia National University, Minia, Egypt
[3] Department of Histology and Cell Biology, Faculty of Medicine, Minia University, 61511, Minia, Egypt
[4] Department of Cardiology, Faculty of Medicine, Minia University, 61511, Minia, Egypt
[5] Department of Medical Physiology, Faculty of Medicine, Aswan University, 81528, Aswan, Egypt
[6] Department of Physiology, RAK College of Medical Sciences, RAK Medical & Health Sciences University, Ras-Alkhaimah 11127, United Arab Emirates
[7] Department of Internal Medicine, Faculty of Medicine, Minia University, 61511, El-Minia, Egypt
[8] Department of Human Anatomy and Embryology, Faculty of Medicine, Aswan University, 81528, Aswan, Egypt
[9] Department of Medical Biochemistry, Faculty of Medicine, Minia University, 61511, El-Minia, Egypt
[10] Department of Biochemistry, Faculty of Medicine, Al-Baha University, Albaha 65525, Saudi Arabia
[11] Department of Surgery, Faculty of Medicine, Aswan University, 81528, Aswan, Egypt
[12] Department of Biochemistry and Molecular Biology, Faculty of Pharmacy, Sohag University, 82524, Sohag, Egypt
[13] Department of Pharmacology and Toxicology, Faculty of Pharmacy, Minia University, 61511, El-Minia, Egypt
[14] Department of Medical Physiology, Faculty of Medicine, Minia University, 61511, El-Minia, Egypt

ARTICLE INFO

Article type:
Original

Article history:
Received:
Accepted:

Keywords:
Endothelial nitric oxide-synthase
Finerenone
Intestinal ischemia-reperfusion
Roflumilast
Vascular endothelial growth-factor

ABSTRACT

Objective(s): Intestinal ischemia is a serious emergency that requires immediate management and surgical intervention. Finding an effective therapeutic strategy, in addition to surgical treatment, is essential to mitigate the harmful effects of intestinal ischemia-reperfusion (IIR)-induced tissue injury not only in the intestine itself but also in distant organs, especially the liver. This prompted us to evaluate, for the first time, the role of finerenone (FIN), a non-steroidal selective mineralocorticoid receptor antagonist, and/or roflumilast (ROF), a selective phosphodiesterase 4 inhibitor, in experimentally induced IIR injury in both hepatic and intestinal tissues, with a detailed study of various mechanisms.

Materials and Methods: Wistar rats were randomly assigned to 5 groups (N=10): Sham group, IIR group, FIN/ROF, FIN, and ROF-administered groups, with IIR induction.

Results: Interestingly, FIN/ROF significantly reduced elevated levels of liver function enzymes, tissue malondialdehyde (MDA), tumor necrosis factor alpha (TNFα), caspase-3 expression, and aldosterone. Furthermore, FIN/ROF could normalize the tissue level of interleukin 10 (IL-10), adenosine monophosphate-activated protein kinase (AMPK), vascular endothelial growth factor (VEGF), endothelial nitric oxide synthase (eNOS), antioxidant parameters, reduced glutathione (GSH), and total antioxidant capacity (TAC) with remarkable improvement in the histopathological features.

Conclusion: FIN/ROF could mitigate IIR-induced hepatic and intestinal damage via FIN-mediated blockade of mineralocorticoid receptors and ROF-mediated inhibition of phosphodiesterase 4, and through antioxidant, anti-apoptotic, and anti-inflammatory properties with regulation of the IL-10/AMPK/VEGF/eNOS pathway. Thus, FIN/ROF is a potential medical treatment for IIR, in addition to surgery.

▶Please cite this article as:
Refaie MMM, Ibrahim RA, Shehata S, Muhammed AA, Elsaghir SMM, Fattah ASMA, Hasan AA, Naiem AHA, Ahmed NZM, Saad MR, Ali DME, Habib HA, Saleh NEH. Efficacy of finerenone and/or roflumilast in alleviation of intestinal ischemic reperfusion injury via regulation of IL10/AMPK/VEGF/eNOS pathway in rats. Iran J Basic Med Sci 2026; 29:

Introduction

Acute intestinal ischemia is a common lethal cause in clinical emergency settings (1). Surgical intervention with adequate restoration of blood supply is mandatory in these cases, simulating a state of intestinal ischemia-reperfusion (IIR) with interrupted blood flow, followed by the excessive release of oxidative and inflammatory agents that circulate throughout the bloodstream. This is caused by acute mesenteric ischemia, septic or hemorrhagic shock, and some surgical procedures like cardiac surgery and abdominal aortic aneurysm, mainly in elderly patients (2, 3). IIR damages the intestinal mucosal barrier, allowing

***Corresponding author:** Amany H. Abdel Naiem. Department of Medical Biochemistry, Faculty of Medicine, Minia University, 61511, El-Minia, Egypt, 14 Faculty of Medicine, Minia National University, Minia, Egypt. Email: amany.haroun@mu.edu.eg

intestinal endotoxins to enter the bloodstream (4). This triggers local and systemic injuries, especially in the liver, brain, testes, or lungs, leading to endotoxemia, systemic inflammatory response, and multiple organ dysfunction (3-6).

The liver is the first organ affected after IIR because of the direct connection between the hepatic and intestinal vasculature, leading to the release of harmful inflammatory and reactive molecules. The gut-liver axis and cytokine cascade also markedly contribute to hepatic injury during IIR (3-5). Restoring blood and oxygen supply during the reperfusion period markedly increases reactive oxygen species (ROS), which can attack all intracellular organelles, resulting in the formation of inflammatory mediators such as interleukins and tumor necrosis factor α (TNFα), followed by stimulation of apoptosis (5-8). Hypoxia-inducible factor (HIF) is a pivotal transcription factor that is stimulated during hypoxic conditions and activates target genes, including vascular endothelial growth factor (VEGF). VEGF is an important signaling protein that can induce vascular growth and act by enhancing endothelial nitric oxide synthase (eNOS) and nitric oxide, with a potent vasodilating impact (9-11). The renin-angiotensin-aldosterone system (RAAS) and adenosine monophosphate-activated protein kinase (AMPK) are also well established as regulators of ischemic injury across different models. Thus, regulating the RAAS and enhancing AMPK activity may have beneficial effects in IIR (12-14). Finerenone (FIN) is a novel non-steroidal agent that blocks mineralocorticoid receptors (MR) and is indicated in chronic renal disease with type 2 diabetes mellitus. Roflumilast (ROF) is another potent, selective inhibitor of the phosphodiesterase-4 enzyme, commonly used in chronic pulmonary diseases. In addition, there is a strong correlation between the actions of FIN and ROF, as both drugs potentiate AMPK and active nucleotides like cAMP that regulate the RAAS system, besides their pleiotropic actions as antioxidants, anti-apoptotic, and anti-inflammatory impacts, with great ability to improve cell oxygenation, blood supply, and to keep cell survival in various models (13, 14). This guided us to elucidate their probable ameliorative effects in IIR. To the best of our knowledge, this is the first research trial to evaluate the novel, alleviating role of FIN/ROF in IIR-induced tissue injury.

Materials and Methods

Animals

Wistar albino rats weighing 180-200 g were obtained from the National Research Center, Giza, Egypt. Rats were allowed free access to a standard diet (chow) and tap water and were left to acclimatize in stainless steel cages. Each cage housed 3-4 rats with regular exposure to a 12-hr dark: light cycle at a temperature of 24±2 ˚C. Approval of this study was obtained from the Care and Use of Laboratory Animals Committee of the Faculty of Medicine, Aswan University (Approval No: Asw.Uni./1087/4/25), in accordance with the EU Directive 2010/63/EU and ARRIVE guidelines for experimental animals. Our data were based on three or more independent experimental observations.

Chemicals

FIN/ROF were from P&C Labs and AstraZeneca Company, Egypt. GSH kits (Cat# GR 2511), and TAC kits (Cat# TA 2513) were from Biodiagnostic Co., Egypt. ELISA kits of ALT, AST, ALP, AMPK and aldosterone (Cat# MBS269614), (Cat# MBS264975), (Cat# MBS165203), (Cat# MBS1602983), (Cat# MBS287151), respectively were from My BioSource Co., San Diego, CA, USA. IL-10 (Abcam, USA, Cat# ab9969), and VEGF (Santa Cruz Biotechnology, USA, Cat# sc-7269). Anti-TNF α antibodies (GeneTex Inc., USA, Cat# GTX54672), activated anti-caspase 3 (Novus Biologicals, UK, Cat# 100-56113), Ready Prep™ protein extraction kit (Bio-Rad Inc., USA, Cat# 163-2086), Bradford Protein Assay Kit (Bio Basic Inc., Canada, Cat# SK3041), β-actin (Elabscience, China, Cat# E-AB-20031), and eNOS marker (Abcam Company, UK, Cat# EPR19945-224) were used.

Experimental design

Grouping of animals

The animals were divided into five groups (n=10). Group 1: Sham group: Animals were given 1 ml of 0.1 % aqueous solution of carboxymethyl cellulose, the vehicle of FIN/ROF, and then were subjected to laparotomy without occlusion of the superior mesenteric artery.

Group 2: IIR group: Rats were given 1 ml of 0.1 % aqueous solution of carboxymethyl cellulose with laparotomy and occlusion of the superior mesenteric artery for 30 min, then reperfusion for 90 min (23).

Group 3: IIR+FIN/ROF: Animals received FIN (10 mg/kg) (24) and ROF (1 mg/kg)(25) orally with laparotomy and occlusion of the superior mesenteric artery for 30 min and reperfusion for 90 min.

Group 4: IIR+FIN: Rats received FIN (10 mg/kg)(24) with laparotomy and occlusion of the superior mesenteric artery for 30 min and reperfusion for 90 min.

Group 5: IIR+ROF: Rats were administered ROF (1 mg/kg) (25) orally with laparotomy and occlusion of the superior mesenteric artery for 30 min and reperfusion for 90 min (23).

FIN/ROF were suspended before their administration in a 0.1% aqueous solution of carboxymethyl cellulose. Choosing the doses was based on the pilot studies and previously published ones.

Steps of surgery

Rats were administered (1 g/kg) a single IP dose of Urethane hydrochloride for induction of general anesthesia, then an abdominal midline incision was performed after sterilization with Betadine. Bulldog clamps were used to occlude the superior mesenteric artery for 30 min as an ischemic period, followed by removal of the clamps to induce reperfusion for 90 min, while maintaining body temperature at 37 ˚C with a heating pad. The same steps were applied to the sham group without vessel occlusion (23).

Sample collection

After the reperfusion period, the animals were sacrificed by cervical dislocation under general anesthesia. Blood was collected from the neck veins, then separated to obtain serum using a centrifuge. For histopathological examination, parts of the small intestine (jejunum) and the liver from each rat were gently excised and fixed in 10 % formalin. Other tissue samples of liver and intestine were immediately frozen in liquid nitrogen, then preserved at -80 ˚C for further biochemical assessments and western

blotting analysis. Tissue homogenization was performed in a 5 ml phosphate buffer solution, and then the mixture was transferred to a test tube for centrifugation at 5000 rpm.

Measuring ALT, AST, ALP, AMPK, and aldosterone

Liver function enzymes (ALT, AST, and ALP), aldosterone, and AMPK were evaluated by ELISA kits according to the manufacturers' instructions. In brief, the microtiter plate of each one was pre-coated with a specific antibody, followed by adding the stored samples or standards to the wells. Each protein was bound to its specific antibody in the pre-coated wells, and sulfuric acid was used to terminate the reaction. Detecting color changes was performed at 450 nm, which was proportional to protein concentration.

Measuring the oxidative stress parameters

Membrane lipid peroxidation was evaluated by measuring thiobarbituric acid reacting substance that is expressed as an equivalent of MDA, using a standard curve of 1,1,3,3-tetramethoxypropane (26). Reduced glutathione (GSH) was also measured by a calorimetric method that depends on the binding of the sulfhydryl group with Ellman's reagent, resulting in the formation of a yellow color detected at 405 nm (27). Also, total antioxidant capacity (TAC) was evaluated calorimetrically at 450 nm.

Histological examination of the hepatic and intestinal tissue

Paraffin preparation with hematoxylin and eosin (H&E) stain

A small segment was excised from the middle part of the jejunum. A 10-cm section was cut from the mid-jejunum, then gently flushed with sterile saline to remove any intestinal content and immediately placed in 10% formalin. After a 24-hr fixation period, jejunum samples were transversely sectioned (~1 cm) at the midpoint. Then both liver and jejunum sections were dehydrated with ethanol, adequately cleared, and placed in paraffin. Sections of 3-4 µm thickness were properly cut from the paraffin-embedded tissues by a rotary microtome, affixed to glass slides, deparaffinized in xylene, rehydrated through a graded ethanol, mounted, and stained with H&E (28, 29).

Periodic acid-schiff reagent (PAS) and alcian blue (AB)

Periodic acid Schiff (PAS) staining was used for examining the content of liver glycogen in hepatocytes and evaluating the cell membrane integrity, and also to visualize the neutral mucins in jejunum sections. In contrast, Alcian blue (AB) was used to localize acidic mucins and assess the presence of goblet cells. Using AB solution (1 g of AB, pH 2.5, 3 ml/l of acetic acid, and 97 ml of distilled water), jejunum tissues were adequately stained with AB and PAS for 30 min. This step was followed by rinsing with tap water for 10 min. For oxidation, PAS (5 g/l) was applied for 5 min, followed by a 10 min tap water rinse, and staining with Coleman's Schiff reagent as a counterstain (Sigma Chemical Co., St. Louis, MO, USA) for 10 min (28, 30).

Immunohistochemical staining of TNFα, caspase 3, and eNOS

Immunohistochemistry staining was applied to sections of 4-5 micrometer thickness. In brief, the sections were adequately deparaffinized, followed by rehydration and rinsing in tap water. The specimens were treated with 3% hydrogen peroxide for 10 min, then immersed in antigen retrieval solution. Nonspecific protein binding was blocked using 10% normal goat serum in phosphate buffer solution. The slides were incubated with the specific antibodies in a 1:1000 dilution, for 18 hr at 4 ˚C in a humid chamber according to the manufacturer's instructions, then with biotinylated secondary antibody, then with streptavidin conjugated to horseradish peroxidase (both from ZymedHistostain-plus-Peroxidase-kit, Cat# 85-9043, San Francisco, CA, USA) for 30 min each. Finally, sections were incubated with diaminobenzidine, and the phosphate buffer solution was used for all dilutions, with washes between stages. Streptavidin peroxidase was added for 10 min, then washed in phosphate buffer solution and counterstained with Mayer's hematoxylin (Zymed Laboratories, USA). After washing with tap water, the sections were dehydrated with a series of graded ethanol, then cleared in xylene and mounted with Entellan (Merck). The same previously described process was applied to negative control samples, except that the primary antibodies were omitted and replaced with phosphate buffer solution alone (28).

Morphometric measurements

The villus height and liver histopathological scoring

The villus height was measured in micrometers from the villus tip to the villus–crypt junction using digital morphometry software (NIH ImageJ software program) to calculate the linear distance from the tip of the intestinal villus down to the villus-crypt junction. Villi heights were measured from 4 complete, vertically oriented villi per slide. A National binocular light microscope (National Optical and Scientific Instruments, Inc., Schertz, TX) was used (31). The histopathological changes in liver tissue were assessed by scoring as follow; 0: minimal injury, grade 1: mild injury manifested as cytoplasmic vacuolization, focal pyknosis, grade 2: moderate obvious injury in form of cytoplasmic vacuolization with no frank necrosis, congestion and sinusoidal dilatation, grade 3: moderate to severe damage with cytoplasmic hypereosinophilia, coagulative necrosis, remarkable sinusoidal dilatation and congestion, grade 4: severe detected injury characterized by severe confluent coagulative necrosis and hemorrhage with loss of hepatic architecture using Image J (FIJI) software. The measurements were done at a magnification of ×400 in ten non-overlapping fields in each rat for each group (32, 33).

Quantitative analysis of caspase 3, TNFα, and eNOS immunohistochemical expression

Histomorphometric analysis was performed using the Leica QWin V.3 program, an image analyzer installed on a computer linked to a Leica DM2500 microscope (Wetzlar, Germany). Measurements were obtained from 3 distinct slides per rat across all groups. From each slide, five independent fields (non-overlapping fields) were carefully examined to find the TNFα and eNOS surface area fraction, and the number of apoptotic cells (positive nuclei) per 1 mm2 and the optical density of caspase-3 expression were measured (X400). The collected morphometric data were analyzed statistically using the Statistical Package for the Social Sciences (SPSS) version 21 (IBM Inc., Chicago, Illinois, USA)(33, 34). The surface area fraction or area percentage means the total tissue that is covered by the brown color reaction to a specific antigen, reflecting how

much of the tissue sample reacts to a specific protein. It is detected by the software Image J. Area fraction %=Area of positive stained /Total area of tissue.

Western blotting analysis of IL10 and VEGF

Following the manufacturer's guidelines, homogenized liver and intestine tissue samples were processed using the ReadyPrep™ protein extraction kit for isolation of total protein. The process of protein quantification was performed using the Bradford Protein Assay Kit according to the provided protocol. Bradford assay analysis was used to determine each sample's protein concentration (35). A total of 20 µg of protein was mixed with an equal volume of Laemmli sample buffer. To ensure proper denaturation, 7.5 µg of each one was heated at 95 ˚C for 5 min in Laemmli buffer (36). A sodium dodecyl sulfate-polyacrylamide gel electrophoresis (SDS-PAGE) was used to separate the proteins, which were then transferred onto Polyvinylidene fluoride membranes. IL10, VEGF, and β-actin antibodies were prepared in Tris-buffered saline with Tween 20 (TBST) according to the manufacturer's instructions. Membranes were incubated overnight with primary antibodies at 4 ˚C, followed by 3-5 washes with TBST for 5 min each (37). Next, membranes were treated with HRP-conjugated secondary antibody (Goat anti-rabbit IgG-HRP, Novus Biologicals) for 1 hr at room temperature, followed by another series of TBST washes. Blocking of the reaction was performed using a 3% bovine serum albumin solution in TBST for 1 hr at room temperature (38). Protein bands were visualized using an enhanced chemiluminescence detection system and captured using a camera-based imaging system. TotalLab software was used to analyze band intensity normalized to the β-actin, then quantified using the ChemiDoc MP imaging system (39).

Statistical analysis of the data

The data were expressed as means +/- (SD), using GraphPad Prism software (version 5.01 for Windows, San Diego, California, USA) for analysis. One-way analysis of variance followed by Tukey's test. *P*-values<0.05 were considered significant.

Results

Effect of FIN/ROF on the liver function enzymes, aldosterone, and AMPK

The untreated IIR group significantly increased liver function enzymes and aldosterone levels but decreased AMPK compared to the sham group and the IIR-treated group (IIR+FIN+ROF). In contrast, co-administration of FIN/ROF alone or in combination significantly decreased the elevated liver enzymes and aldosterone levels, but increased AMPK compared to the IIR-untreated group (Table 1).

Evaluation of oxidative stress measurements (MDA, GSH, TAC)

There were elevations in MDA tissue levels but a decrease in GSH and TAC levels in the IIR group of the examined tissues when compared to the sham group and the IIR-treated group (IIR+FIN+ROF). Co-administration of FIN/ROF reversed these changes when compared to the IIR-untreated group (Table 2).

Table 1. Effect of FIN/ROF on rat liver enzymes, aldosterone, and AMPK in the IIR model

Groups	ALT (U/L)	AST (U/L)	ALP (U/L)	AMPK (ng/ml)	Aldosterone (Pg/ml)
Sham	1.1±0.3	1.2±0.3	2.0±0.9	10.1±0.7	2.0±0.2
IIR	8.3±1.1ab	7.9±1.6ac	58.5±11.9ac	3.8±0.2ac	13.9±0.8ac
IIR+FIN+ROF	3.9±0.9ab	4.6±0.9ab	15.8±4.6ab	8.8±0.6ab	4.1±0.3ab
IIR+FIN	6.2±1.1abc	5.4±1.7ab	26.2±5.2abc	5.9±0.4 abc	7.9±0.4abc
IIR+ROF	6.7±1.2abc	6.3±1.4ab	22.7±4.2abc	6.0±0.5 abc	6.6±0.3abc

Data are presented as means±SD for 10 observations per group. Differences were considered statistically significant when the *P-value* was less than 0.05. a Significant compared to the sham group; b Significant compared to the IIR group; c Significant compared to the finerenone- and roflumilast-treated group
FIN: Finerenone, ROF: Roflumilast, IIR: Intestinal ischemia-reperfusion-induced group, ALT: Alanine aminotransferase, AST: Aspartate aminotransferase, ALP:Alkaline phosphatase, AMPK: adenosine monophosphate- activated protein kinase

Table 2. Effect of FIN/ROF on rat oxidative stress parameters

Groups	Intestine GSH (µmol/g tissue)	Intestine MDA (nmol/g tissue)	Hepatic GSH (µmol/g tissue)	Hepatic MDA (nmol/g tissue)	TAC (mmol/l)
Sham	469.0±68.2	33.3±7.4	484.0±98.7	31.9±6.6	0.9±0.06
IIR	159.4±40.6ac	89.3±12.7ac	156.4±39.2ac	90.0±14.8ac	0.4±0.2ac
IIR+FIN+ROF	393.4±48.5ab	27.6±5.8b	406.4±44.4ab	28.2±4.3ab	0.7±0.05b
IIR+FIN	231.2±44.9ac	79.1±8.8ac	238.0+48.3ac	77.1±8.5abc	0.5±0.01abc
IIR+ROF	266.2±42.4ac	75.3±6.4ac	263.2+37.2ac	72.4±9.9ac	0.6±0.1ac

Data are presented as means±SD for 10 observations per group. Differences were considered statistically significant when the *P-value* was less than 0.05. a Significant compared to the sham group; b Significant compared to the IIR group; c Significant compared to the finerenone- and roflumilast-treated group
FIN: Finerenone, ROF: Roflumilast, IIR: Intestinal ischemia-reperfusion-induced group, GSH: Reduced glutathione, MDA:malondialdehyde

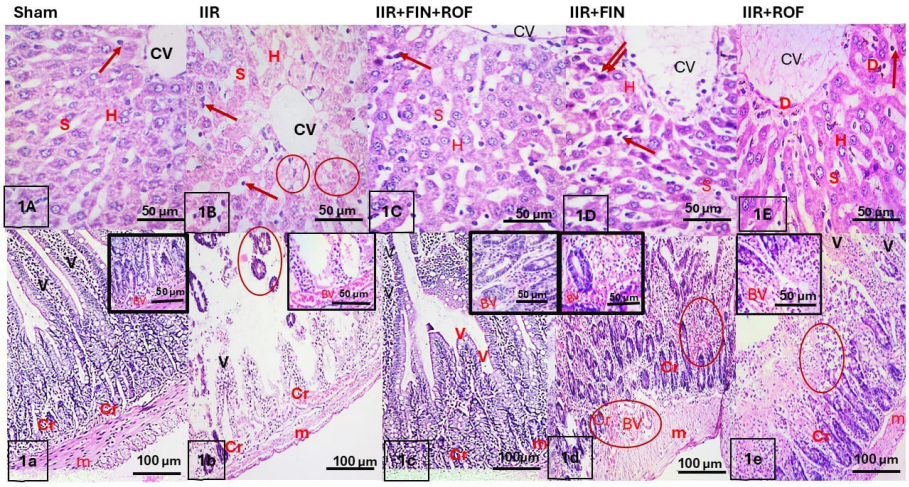

Figure 1. H&E staining of liver sections in different rat groups
A, C showing the central vein (CV) surrounded by cords of hepatocytes (H) with round vesicular nuclei and prominent nucleoli. Notice, hepatic sinusoids (S) are lined with Kupffer cells (red arrows). Apparent uniform acidophilic staining of the cytoplasm. B shows degenerated liver cells with apparent pale acidophilic cytoplasm. Notice, some cells show vacuolated cytoplasm with apoptotic nuclei (circle). D, E show congestion and dilatation of the central vein and hepatic sinusoids with areas of strongly hepatocytic acidophilic cytoplasm (double arrows) with pyknotic nuclei. Notice some black dust-like cells scattered around CV and in hepatic sinusoids (D).
H&E staining of the jejunum of different rat groups
The mucosa consists of villi (V) and crypts (Cr). Inset showing submucosa contains blood vessels (BV), Muscularis externa
1- (m) inner circular, outer longitudinal fibers.
a, c show the normally arranged structure of villi and crypts. b shows most of the degenerated mucosa with ghosts of villi and remnant crypts. Some crypts appear exfoliated from the mucosa (*). Notice, some blood vessels appear congested in the submucosa and between villi and crypts (inset). d, e show many preserved crypts and loss of many villi, which were replaced by high infiltrations of inflammatory cells (mainly polymorphonuclear cells and lymphocytes) in the upper mucosal surface. Notice, many congested dilated blood vessels and extravasation of some blood vessels, especially at the superficial layer of mucosa and between crypts (circle). H&E (1A, B, C, D, E & inset x400)-(1a, b, c, d, e x 10)
H&E: Hematoxylin and Eosin staining, CV: Central Vein, H: Hepatocytes, S: Hepatic Sinusoids, BV: Blood Vessels, V: Villi, Cr: Crypts, m: Muscularis externa (inner circular and outer longitudinal fibers)

Histopathological findings

Routine microscopic findings

Liver: In Figure 1, the sham and IIR+FIN+ROF groups appear with normal architecture in the form of a central vein surrounded by hepatocytes arranged in cords with round vesicular nuclei, prominent nucleoli, and the sinusoids are lined with Kupffer cells (Figure 1A, C). IIR group showed degenerated hepatocytic cells with apparent pale acidophilic cytoplasm, and some cells showed vacuolated cytoplasm (Figure 1B). IIR+FIN and IIR+ROF groups appeared with congestion and dilatation of the central vein and hepatic sinusoids, with areas of acidophilic cytoplasm, pyknotic nuclei, and some dust-like cells surrounding the CV and in the hepatic sinusoids. The appearance of many dust-like cells may indicate an increase in both Kupffer cells and hepatic Stellate cells (Ito cells) activity. Stellate cells are star-shaped cells located in the space of Disse, present in the tiny perisinusoidal space that surrounds the sinusoids and liver cells. They appeared in a somewhat dust-like shape. (Figure 1D, E).

Jejunum: In Figure 1, the sham and IIR+FIN+ROF groups appeared in normally arranged layers with mucosa containing both villi and crypts. Submucosa had some blood vessels, and the muscularis externa appeared with a normal arrangement of smooth muscle fibers in the form of inner circular and outer longitudinal fibers (Figure 1a, c). IIR group showed a loss of the general architecture of the mucosa in the form of degenerated villi and crypts, which are not observed in the sham group. Certain regions of the exfoliated crypts were found away from the mucosa. Some blood vessels appeared congested in the submucosa, between the villi and crypts (Figure 1b). IIR+FIN/ROF groups showed many preserved crypts with loss of many villi, which were replaced by intense infiltrations of inflammatory cells (mainly polymorphonuclear cells and lymphocytes) and congested dilated blood vessels, especially at the superficial layer of mucosa (Figure 1d, e).

PAS -Alcian blue results

Liver: All groups except the IIR group showed a strong PAS magenta red glycogen granulation reaction in the cytoplasm of most cells with preserved architecture of their cell membranes. While the IIR group appeared with a faint, weak PAS-positive reaction in most of the hepatocytes, which appeared in degenerated architecture with lost continuity of their cell membranes (Figure 2).

Jejunum: Strong bluish coloration reaction of mucin production of goblet cells at the levels of villi and crypts was observed in both sham and IIR+FIN+ROF groups. In comparison, the IIR group showed a negative reaction in villi and a weak reaction in remnant crypts. IIR+FIN and IIR+ROF groups showed moderate bluish coloration reaction of mucin production of goblet cells in most crypts (Figure 2).

Immunohistochemical results

eNOS immunohistochemical results

Liver: Sham and IIR+FIN+ROF groups showed strong positive eNOS expression in the endothelium lining of the central vein, in the cytoplasm of most hepatocytes, especially around central veins, and in the endothelium of hepatic sinusoids. Compared with previous groups, the IIR group showed a faint, weak positive-to-negative reaction in most hepatocytes, especially around central veins and in some areas of hepatic sinusoids in degenerated hepatocytes. In contrast, IIR+FIN and IIR+ROF groups showed moderate to weak cytoplasmic positive reaction in most of the hepatocytes, especially around central veins (Figure 3).

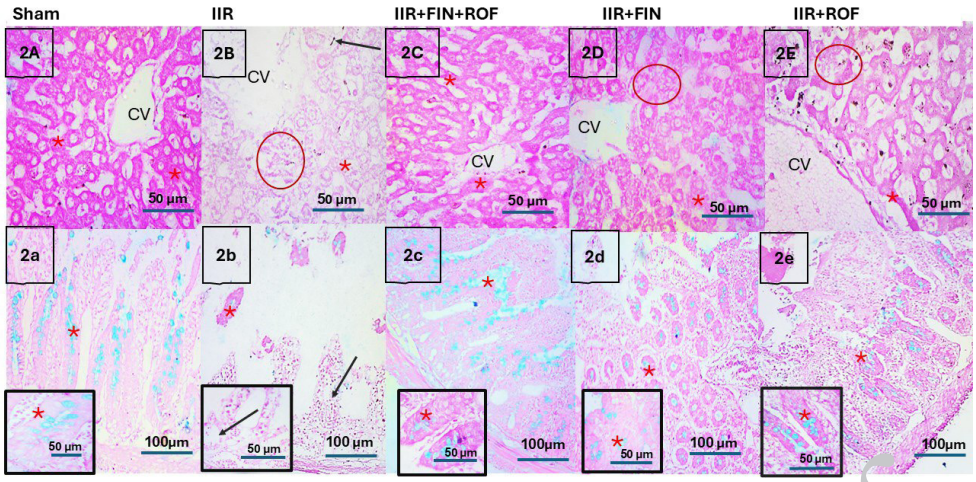

Figure 2. PAS staining of liver sections in different rat groups showing the central vein (C) surrounded by cords of hepatocytes (H)
I-A, C, D, E showing dispersed strong reaction (magenta red reaction glycogen granulations) in the cytoplasm of most liver cells (*), especially around central veins and the endothelium lining of sinusoids. Notice that some regions appear with weak reactions (circles). B shows a faint PAS reaction in most hepatocytes (*). Notice, degenerated hepatocytic architecture with lost continuity of cell membranes (circle)
PAS-Alcian blue staining of the jejunum in different rat groups
a strong bluish coloration (PAS-AL) reaction (*) of mucin of goblet cells (insets) and in many areas of both segments (villi+ crypts) (inset). b a negative reaction (PAS-AL) in remnants of villi (inset-*) and a weak reaction in crypts (*). d, e bluish coloration reaction of mucin of goblet cell (insets) in many regions (*-insets) of villi and crypts (PAS- Alcian blue, (2A, B, C, D, E & inset x400)-(2a, b, c, d, e x 10)
PAS: Periodic acid–Schiff staining, PAS-AL: Periodic acid–Schiff–Alcian blue staining, C: Central Vein, H: Hepatocytes

Jejunum: Results of rat jejunum sections immunohistochemically stained for eNOS of sham and IIR+FIN+ROF groups showed moderate to strong positive reaction in most of the endothelial cells between crypts and villi core. Many areas of nuclear and cytoplasmic reaction in the submucosa were observed. The IIR group showed a faint weak nuclear reaction between remnants of crypts. At the same time, both the IIR+ FIN and the IIR+ROF groups showed moderate positive nuclear reaction in all cells, especially between crypts and remnants of villi. Many weak positive nuclear and cytoplasmic reactions were observed in the submucosal areas (Figure 3).

TNFα immunohistochemical results in hepatic and intestinal tissues

There is a positive cytoplasmic reaction of TNFα in the IIR group compared to the sham group and the IIR+FIN+ROF groups in both hepatic and intestinal tissues. Some nuclear reactions were also observed in hepatic cells, including von Kupffer cells, endothelial cells, and cells lining blood sinusoids, as well as in the intestinal stroma. IIR+FIN and IIR+ ROF groups showed positive cytoplasmic and nuclear

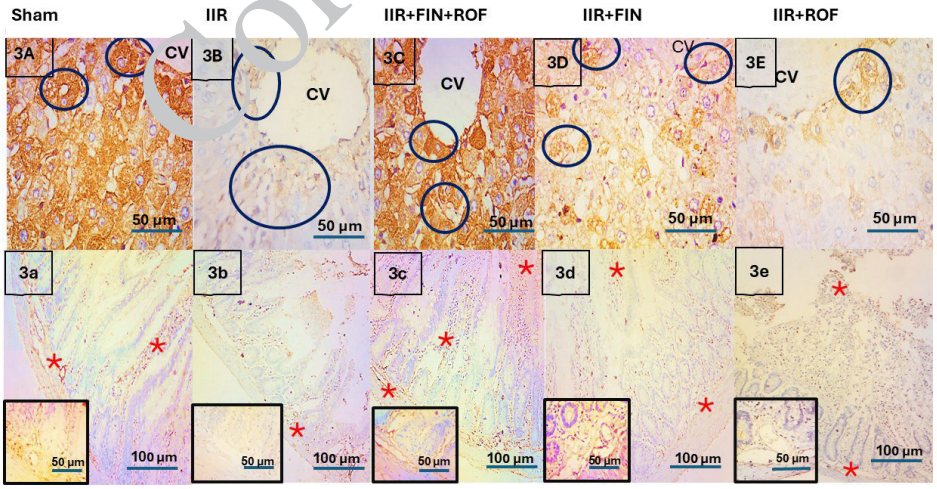

Figure 3. Immunohistochemical staining of rat liver sections for eNOS showing the central vein (C) surrounded by cords of hepatocytes (H)
I- A, C show strong reaction (brown coloration) in the cytoplasm of most hepatocytes, especially around the endothelium of central veins and the endothelium of hepatic sinusoids (circle). B shows a faint, weak positive to negative reaction in most hepatocytes, especially around the central veins (small circle). Notice a faint reaction between degenerated hepatocytes with lost continuity of cell membranes (large circle). D, E show a weak positive to negative cytoplasmic reaction in most of the hepatocytes, especially around central veins and endothelium lining central veins and hepatic sinusoids (circle)
II-: Immunohistochemical staining of rat jejunum sections for eNOS in different groups
a, c showing strong positive reaction in blood vessel lining cells between crypts and core of villi (*). Notice, many nuclear and cytoplasmic reactions in submucosa areas lining the endothelium of blood vessels (inset). b shows a faint weak nuclear reaction between remnants of crypts. d, e positive nuclear reaction in all cells, especially between crypts and ghosts of villi and upper mucosal areas (*). Notice, weak positive nuclear and cytoplasmic reaction in submucosal areas (inset). (IHC- eNOS (3A, B, C, D, E &inset x400)-(3a, b, c, d, e x10)
IHC: Immunohistochemical staining, eNOS: Endothelial Nitric Oxide Synthase, C: Central Vein, H: Hepatocytes

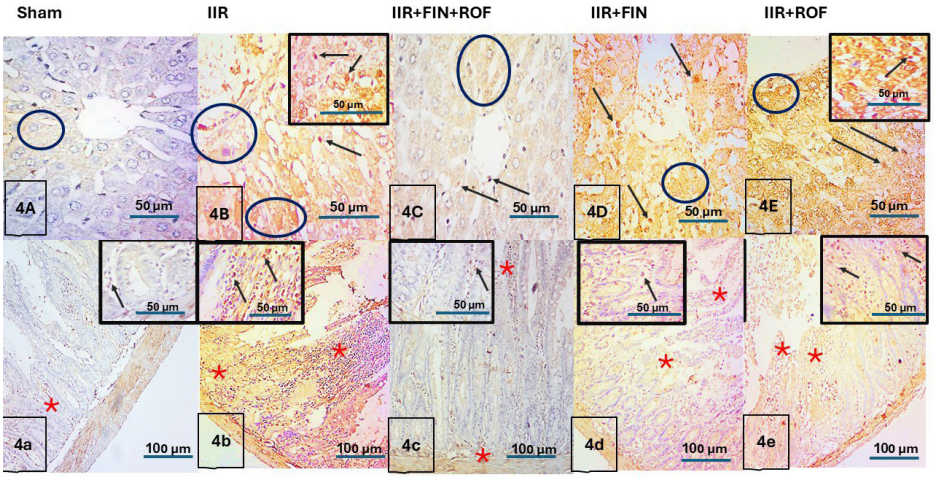

Figure 4. Immunohistochemical staining of rat liver sections for TNFα showing the central vein surrounded by cords of hepatocytes
I-A, C showing negative to weak cytoplasmic reaction (circle) in most of the hepatocytes, especially around the central veins. Notice a few scattered nuclear reactions in the cells (black arrow). B shows a strong positive reaction in most of the cytoplasm of all hepatocytes, especially around the central veins (circle). Notice that many nuclear reactions occur within and between cells (black arrows, inset). D, E show a strong positive reaction in most of the cytoplasm of hepatocytes, especially around the central veins (circle). Notice, many nuclear reactions in the cells (black arrows- inset)
II-Immunohistochemical staining of rat jejunum sections for TNFα
Figure 4 a, c negative to faint weak cytoplasmic reaction in most of the cells of the villus epithelium (*). Notice, scatter a few nuclear reactions in the core of the villi and in between crypts (black arrows-inset). Figure 4b shows strong positive cytoplasmic and nuclear reaction in most of the cells in the cores of ghosts villi (*) and in between crypts (black arrows- inset). d, e positive reaction in all cells, especially in the remnant core of villi and upper regions of mucosa (*). Notice that many nuclear reactions are scattered between crypts (black arrows, inset). (TNF- IHC (4 A, B, C, D, E & inset x400)-(4a,b,c,d,e x 10)
IHC: Immunohistochemical staining, TNFα: Tumor Necrosis Factor Alpha, CV: Central Vein

reactions in some cells (hepatic cells, cell lining villi, crypts, and in the stroma of the intestine). The sham group showed a very faint reaction, and weak nuclear and cytoplasmic reactions were observed in some areas in the IIR+FIN+ROF group (Figure 4).

Caspase3 immunohistochemical results in hepatic and intestinal tissue

The IIR group showed a strong positive cytoplasmic caspase-3 reaction compared with the sham group and the IIR+FIN+ROF groups in both hepatic and intestinal tissues. Many nuclear reactions were also observed scattered in the hepatocytes of liver tissue, inside them, and in the stroma of the intestine. IIR+FIN and IIR+ROF groups showed positive cytoplasmic and nuclear reactions in the hepatic cells, including the cell lining villi, crypts, and scattered in the stroma of the intestine. While the sham group showed a very faint reaction, some areas of weak nuclear and cytoplasmic reactions were observed in the IIR+FIN+ROF group (Figure 5).

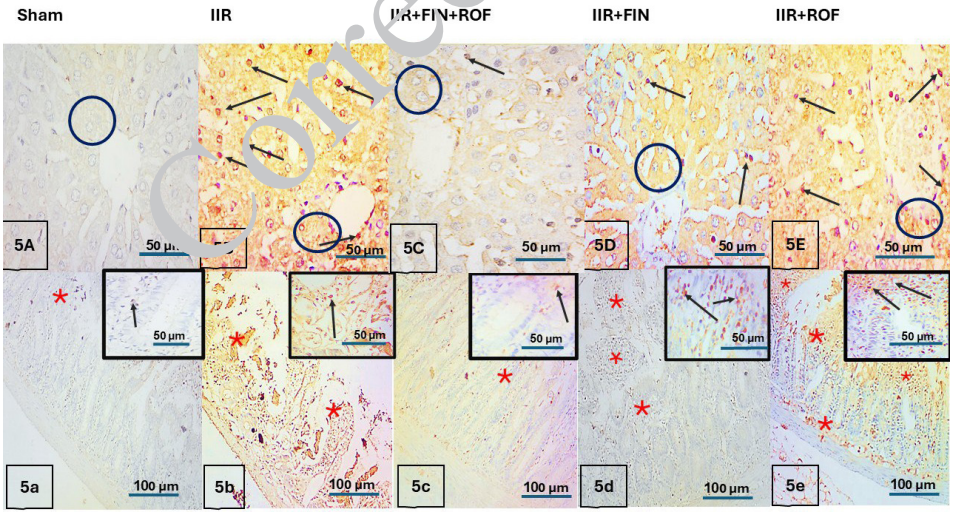

Figure 5. Immunohistochemical staining of rat liver sections for cleaved caspase 3 showing the central vein surrounded by hepatocyte cords
I- A, C showing negative to weak cytoplasmic reaction (circle) in most of the hepatocytes, especially around the central veins. Notice, scatter a few nuclear reactions in cells (black arrows). B shows a strong positive reaction in most of the cytoplasm in all hepatocytes, especially around the central veins (circle). Notice that many nuclear reactions appear in and between cells (black arrows). D, E show a positive reaction in most of the cytoplasm of hepatocytes, especially around the central veins (circle). Notice some nuclear reactions in and between cells (black arrows)
II-Immunohistochemical staining of rat jejunum sections for cleaved caspase 3
a, c showing negative to faint weak cytoplasmic and nuclear reaction in most of the cells, especially lining villi and core connective tissue (*). Notice a few scattered nuclear reactions in between crypts (black arrows- inset). b a strong positive cytoplasmic reaction in most cell-lining ghosts of villi and remnant crypts (*). Notice, many nuclear reactions in between remnants of villi and crypts (black arrows- inset). A positive cytoplasmic reaction in all cells, especially in the lining of the upper mucosa (*). Notice, many nuclear reactions in between crypts at remnants of villi (black arrows- inset) (Caspase 3- IHC, (5A, B, C, D, E & inset x400,)-(5 a, b, c, d, e x 10)
IHC: Immunohistochemical staining

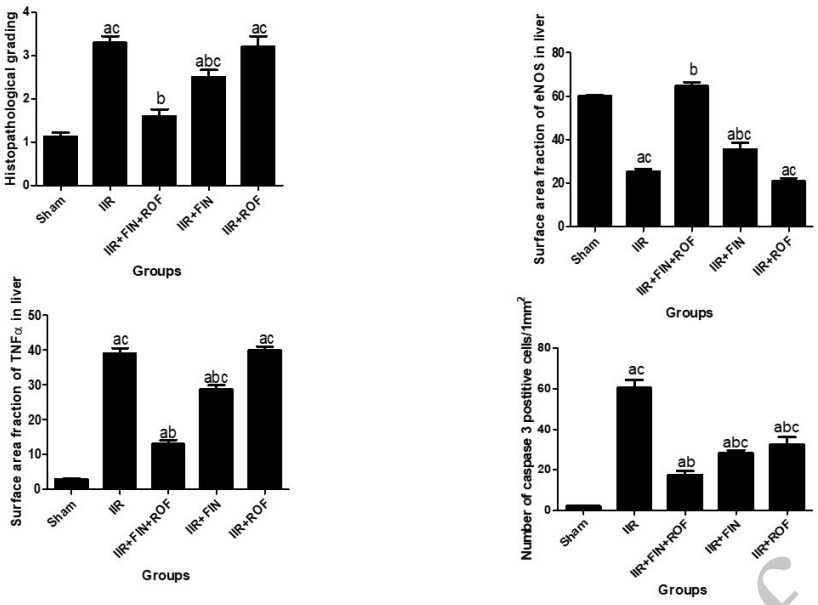

Figure 6. Morphometric analysis of rat liver tissue
There was a significant increase in the number of cleaved caspase-3 positive cells, TNFα immune expressions, and hepatic injury score, but decrease in eNOS immune expression in the untreated ischemic group, compared to the sham group and the IIR+ FIN+ROF group. Nevertheless, co-administration of FIN+ROF could decrease the number of cleaved caspase-3 positive cells, TNFα immune expressions, hepatic injury score, but increase eNOS immune expression in the treated ischemic group compared to the untreated ischemic group
Data are presented as means±SD for 10 observations per group. Differences were considered statistically significant when the *P-value* was less than 0.05.) a Significant compared to the sham group; b Significant compared to the IIR group; c Significant compared to the finerenone- and roflumilast-treated group
FIN: Finerenone; ROF: Roflumilast. IIR: Intestinal ischemia-reperfusion-induced group, TNFα: Tumor Necrosis Factor Alpha, eNOS: Endothelial Nitric Oxide Synthase, SD: Standard Deviation

Morphometric analysis

The histopathological changes in the hepatic tissue of the IIR group showed a significant increase in the scoring of damage graded as 4 in the form of cytoplasmic vacuolization, focal pyknosis, congestion, and sinusoidal dilatation observed in many areas of liver tissue, when compared to the sham group. Using FIN/ROF alone or in combination showed improvement in the histopathological scoring when compared to the IIR group. The use of FIN/ROF alone was graded as 2 or 3, but their combination was graded as 1 or 2.

Data revealed significant increases in the number of cleaved caspase-3-positive cells, TNF-α expression, and scores of hepatic and intestinal injury, but decreases in eNOS immune expression and Villus height in the IIR group compared with the IIR+FIN+ROF and sham groups. However, FIN/ROF received groups could decrease the number of cleaved caspase-3 positive cells, TNFα immune expressions, score of hepatic and intestinal injury, but increase Villus height in um and eNOS immune expression in comparison with the untreated group (Figures 6 and 7).

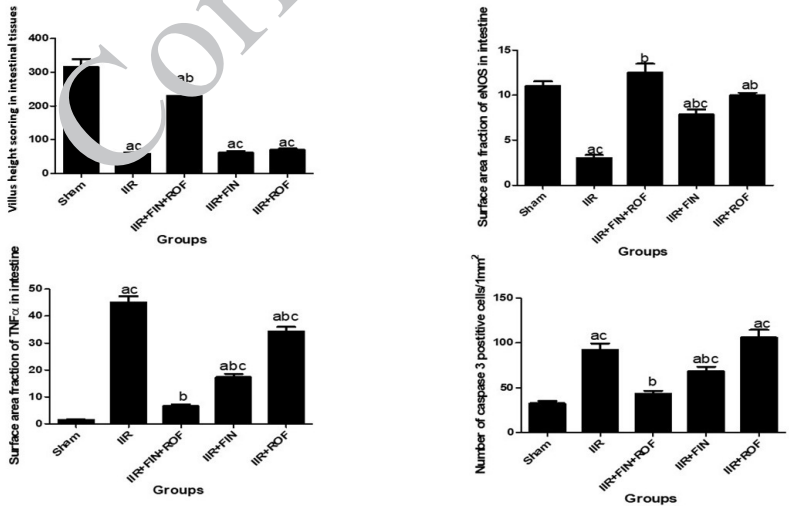

Figure 7. Morphometric analysis of rat intestinal tissue
Data revealed significant increases in cleaved caspase-3 and TNFα immune expressions but decreases in eNOS immune expression and intestinal Villus height in (um) in the ischemic untreated group, co-administered groups, when compared to the sham group, and the IIR+ FIN+ROF treated group. However, the FIN+ROF-treated group could decrease cleaved caspase-3 and TNFα immune expressions but increase eNOS immune expression and intestinal Villus height in (um) if compared to the untreated ischemic group.
Data is presented as means±SD for 10 observations per group. Differences were considered statistically significant when the *P-value* was less than 0.05.) a Significant compared to the sham group; b Significant compared to the IIR group; c Significant compared to the finerenone- and roflumilast-treated group
FIN: Finerenone; ROF: Roflumilast. IIR: Intestinal ischemia-reperfusion-induced group, TNFα: Tumor Necrosis Factor Alpha, eNOS: Endothelial Nitric Oxide Synthase, SD: Standard Deviation

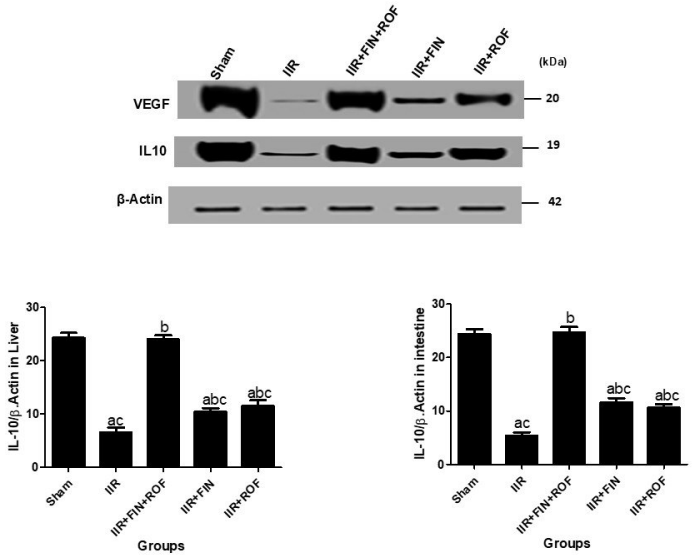

Figure 8. Western blotting analysis of IL10
Hepatic and intestinal tissue had a significant decrease of IL10 in the IIR untreated group, when compared to the sham group and the IIR+ FIN+ROF group. Nevertheless, IL10 significantly increased in the FIN+ROF-treated group when compared to the IIR untreated group. Data are presented as means±SD for 10 observations per group. Differences were considered statistically significant when the *P-value* was less than 0.05. a Significant compared to the sham group; b Significant compared to the IIR group; c Significant compared to the finerenone- and roflumilast-treated group
FIN: Finerenone; ROF: Roflumilast. IIR: Intestinal ischemia-reperfusion-induced group, IL10: Interleukin-10, SD: Standard Deviation

Western blotting analysis of IL10 and VEGF

IL10 and VEGF were significantly diminished in the IIR-untreated group compared with the sham group and the IIR-treated group (IIR+ FIN+ROF). However, their expressions are improved upon co-administration of FIN+ROF. These findings were detected in both hepatic and intestinal tissue samples (Figures 8 and 9).

Discussion

Intestinal ischemia-reperfusion (IIR) is associated with noticeable local and systemic pathological consequences mediated by oxidative stress, inflammatory cascades, and microvascular dysfunction. Moreover, restoration of the blood flow following ischemia results in more mucosal and endothelial damage. These events negatively affect the intestinal barrier integrity and promote bacterial translocation, which subsequently triggers a systemic inflammatory response in the remote highly vascularized organs, especially the liver (1-3, 25, 40, 41). Thus, the current model was performed, which revealed significant elevations in the liver function enzymes (ALT, AST, ALP), MDA, caspase-3, aldosterone, and TNFα in the IIR group in both the intestinal and hepatic tissues. However, TAC and GSH significantly diminished with obvious disturbances in

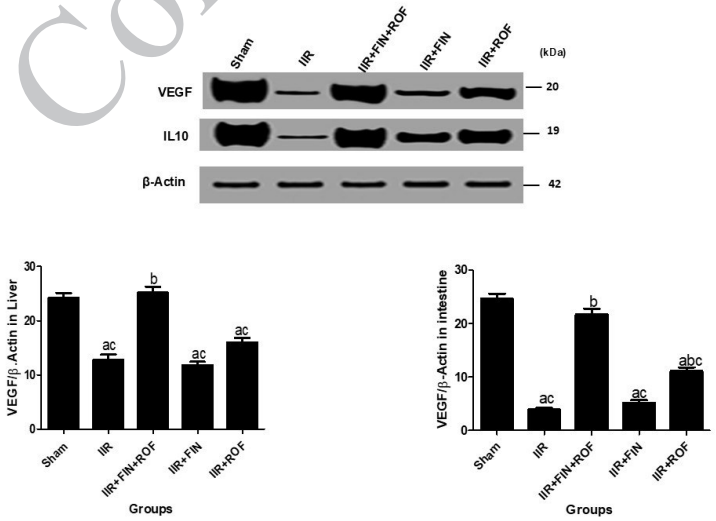

Figure 9. Western blotting analysis of vascular endothelial growth factor (VEGF) in rats
Intestinal and hepatic tissues showed a significant decrease in VEGF in the IIR untreated group, when compared to the sham group and the IIR+ FIN+ROF groups. However, it significantly increased in the FIN+ROF-treated group, compared to the IIR-untreated group. Data are presented as means±SD for 10 observations per group. Differences were considered statistically significant when the *P-value* was less than 0.05. a significant compared to the sham group; b Significant compared to the IIR group; c Significant compared to the finerenone- and roflumilast-treated group
FIN: Finerenone; ROF: Roflumilast. IIR: Intestinal ischemia-reperfusion-induced group, SD: Standard Deviation

the histopathological features and abnormal IL10/AMPK/VEGF/eNOS signaling cascade. Fortunately, the FIN/ROF-treated group could decrease liver enzyme levels, improve the histopathological features, diminish MDA, caspase-3, aldosterone, and TNFα, but increase TAC and GSH with anti-inflammatory, anti-oxidant, and anti-apoptotic properties.

Different mechanisms are responsible for IIR-induced injury, especially oxidative stress with excessive release of ROS that attack intracellular molecules, disturb the dynamic homeostasis, negatively affect the epithelial cells, cause membrane lipid peroxidation, mitochondrial dysfunction, initiate different inflammatory pathways with excessive production of the inflammatory mediators such as TNFα, leading to stimulation of the apoptotic signaling (7, 40-42). This explains the oxidative imbalance detected in the IIR group, as evidenced by elevated MDA levels and depletion of GSH and TAC, supporting the critical contribution of oxidative stress. In contrast, FIN/ROF co-treatment markedly attenuated lipid peroxidation and restored the antioxidant defense, indicating effective limitation of oxidative tissue damage, as the results showed decreased MDA levels but increased GSH and TAC. Greater protection was observed in the combined treatment compared with monotherapy, suggesting complementary pharmacological actions between FIN and ROF against IIR injury (42-44). This is in accordance with previous studies supporting our findings (21-25).

Current results also detected elevations of TNFα and caspase-3 expressions, and aldosterone levels, but decreased AMPK, supporting the involvement of RAAS, inflammatory, and apoptotic pathways in IIR (44-47). This could be explained by the recent detection of more advanced complex players in ischemic disorders, as enhancing AMPK, cAMP, and cGMP, and suppressing RAAS overactivity and MR could mitigate ischemic damage (6, 40-42). Besides, the apoptotic process has a central role in mediating IIR injury as there is a cross-link between mitochondrial damage and the release of various pro-apoptotic factors, triggering activation of caspase-9, which in turn enhances caspase-3 induced apoptotic action (6,38-42). In addition, neutrophils and activated Kupffer cells associated with the release of oxygen free radicals and inflammatory cytokines, including IL6 and TNFα, are highly involved in IIR (44-47). Conversely, FIN or ROF administration markedly improved tissue architecture and reduced apoptotic burden, indicating suppression of inflammation-associated cell death with tissue preservation. This could also be explained by FIN's ability to block MR. In addition, ROF enhances cAMP formation, the main regulator and protector of vascular and tissue injury during ischemia. Furthermore, FIN and ROF have anti-inflammatory, anti-fibrotic, anti-apoptotic, and anti-oxidant effects with vasodilation (15-20).

Histopathological results in the IIR group revealed degeneration in both cellular morphology and function, impacting the villi height in the intestine, and decreasing the production of glycogen contents in the hepatocytes and goblet cells in the intestinal villi and crypts. Besides that, it had a detrimental effect on cell membrane integrity in both hepatocytes and the epithelium lining the intestinal mucosa. These observations could be explained as in ischemic conditions, eNOS formation decreases, accompanied by a deficiency of nitric oxide, impairing epithelial differentiation and mucus production (15-22, 48-53). This is in line with current findings of immunohistochemical and morphometric analysis.

Another important finding in the current work is the reduction of IL10 and VEGF expression in untreated IIR animals, accompanied by suppression of AMPK and eNOS. Since IL10 is a critical endogenous anti-inflammatory mediator that limits cytokine-induced tissue injury, and VEGF contributes to endothelial maintenance and tissue repair. Furthermore, IL10 could stimulate the AMPK/VEGF/eNOS axis for further protection of the endothelial cells. The restoration of the IL10/AMPK/VEGF/eNOS axis following FIN/ROF administration suggests broader cytoprotective effects beyond the control of inflammation alone, constituting an important mechanistic pathway during IIR. This crosstalk between IL10 and the AMPK/VEGF/eNOS signaling cascade, as a protective mechanism, was previously confirmed in various models (54-59). Taking all findings in our study together, it is evident that FIN/ROF have protective impacts that contribute to the amelioration of IIR-induced injury. This is due to the antioxidant, anti-apoptotic, and anti-inflammatory properties of FIN and ROF, along with modulation of the IL10/AMPK/VEGF/eNOS signaling pathway. In addition, FIN works by blocking MR, while ROF primarily inhibits phosphodiesterase-4 and increases cAMP. Overall, FIN/ROF may be a promising adjunctive therapy for IIR, alongside surgical intervention. Current research paves the way in considering FIN/ROF as an adjuvant medical treatment in alleviating intestinal and hepatic injury during IIR.

Conclusion

Co-administration of FIN/ROF succeeded in decreasing IIR, mostly depending on its ability to inhibit MR by FIN and increase cAMP by ROF, with regulation of the IL10/AMPK/VEGF/eNOS pathway, antioxidant, anti-apoptotic, and anti-inflammatory properties, and amelioration of the histopathological changes of both liver and intestine. Further studies are really needed to evaluate this effect in patients with intestinal ischemia.

Study limitations

This research is limited to studying the ameliorative effect of FIN+ROF on human cells and evaluating their roles in clinical settings.

Acknowledgment

We'd like to acknowledge AstraZeneca Company for their generous help and cooperation to this research.

Funding

This study is self-funded; no specific grants were received from any funding agencies in the public, commercial, or not-for-profit sectors

Data Availability Statement

Data is available upon request

Authors' Contributions

MMM R, S S, AA M, ASMA F, SMM E, AA H, MR S, DME A, AHA N, HA H, and NEH S were responsible for conceptualization, methodology, data curation, formal analysis, resources, software, supervision, and writing,

including the original draft, review, and editing. AA H contributed to part of the H&E histopathological evaluation. RA I handled the methodology, execution, writing, review, and editing of the histopathology and immunohistochemistry sections, as well as the statistical analysis and manuscript revision. NZM A and DME A managed the methodology, execution, writing, review, and editing of the Western blotting section. MMM R selected key points, authored, and revised the manuscript. All authors have read and approved the final version.

Conflicts of Interest

The authors declare no conflicts of interest.

Declaration

We have not used any AI tools or technologies to prepare this manuscript.

References

1. Neha K, Haider MR, Pathak A, Yar MS. Medicinal prospects of antioxidants: A review. Eur J Med Chem 2019; 178: 687-704.
2. Jing HR, Luo FW, Liu XM, Tian XF, Zhou Y. Fish oil alleviates liver injury induced by intestinal ischemia/reperfusion via AMPK/SIRT-1/autophagy pathway. World J Gastroenterol 2018; 24: 833-843.
3. Wang Y, Wen J, Almoiliqy M, Wang Y, Liu Z, Yang X, *et al.* Sesamin protects against and ameliorates rat intestinal ischemia/reperfusion injury with involvement of activating Nrf2/HO-1/NQO1 signaling pathway. Oxid Med Cell Longev 2021; 2021: 5147069.
4. Olivero C, Carbone F, Liberale L, Montecucco F. Precision medicine in intestinal ischemia: the emerging role of biomarkers. Intern Emerg Med 2025; 20: 369-379.
5. Li G, Wang S, Fan Z. Oxidative stress in intestinal ischemia-reperfusion. Front Med 2022; 8: 750731.
6. Zhao T, Lu J, Qin J, Chen Y, Shi Z, Wei W, *et al.* Altered intestinal barrier contributes to cognitive impairment in old mice with constipation after sevoflurane anesthesia. Front Nutr 2023; 10: 1117028.
7. Korkmaz A, Oyar E, Yildirim Z, Pampal A, Unlu N, Akbulut H. Application of vascular endothelial growth factor at different phases of intestinal ischemia/reperfusion: What are its effects on oxidative stress, inflammation and telomerase activity? Adv Clin Exp Med 2020; 29: 1417-1424.
8. Chai D, Zhang L, Xi S, Cheng Y, Jiang H, Hu J. Nrf2 activation induced by Sirt1 ameliorates acute lung injury after intestinal ischemia/reperfusion through NOX4-mediated gene regulation. Cell Physiol Biochem 2018; 46: 781-792.
9. Bosma EK, Darwesh S, Habani YI, Cammeraat M, Serrano Martinez P, van Breest Smallenburg ME, *et al.* Differential roles of eNOS in late effects of VEGF-A on hyperpermeability in different types of endothelial cells. Sci Rep 2023; 13: 21436.
10. Wang Y, Gao H, Cao X, Li Z, Kuang Y, Ji Y, *et al.* Role of GADD45A in myocardial ischemia/reperfusion through mediation of the JNK/p38 MAPK and STAT3/VEGF pathways. Int J Mol Med 2022; 50: 144.
11. Ozden ES, Ozcan MS, Ilhan I, Tepebasi MY, Taner R, Uysal D, *et al.* Radiofrequency electromagnetic field ınhibits HIF-1 alpha and activates eNOS signaling to prevent intestinal damage in a model of mesenteric artery ischemia in rats. Int J Med Sci 2025; 22: 1465.
12. Blikslager AT, Roberts MC, Young KM, Rhoads JM, Argenzio RA. Genistein augments prostaglandin-induced recovery of barrier function in ischemia-injured porcine ileum. Am J Physiol Gastrointest Liver Physiol. 2000; 278: G207-216.
13. Govender D, Damjanovic L, Gaza CA, Meyer V. Vitamin D decreases silencer methylation to downregulate renin gene expression. Gene 2021; 786: 145623.
14. Khedr RM, Ahmed AAE, Kamel R, Raafat EM. Sitagliptin attenuates intestinal ischemia/reperfusion injury via cAMP/PKA, PI3K/Akt pathway in a glucagon-like peptide 1 receptor-dependent manner. Life Sci 2018; 211: 31-39.
15. Ou C, Lin Y, Wen J, Zhang H, Xu Y, Zhang N, *et al.* Roflumilast attenuates microglial senescence and retinal inflammatory neurodegeneration post retinal ischemia reperfusion injury through inhibiting NLRP3 inflammasome. Invest Ophthalmol Vis Sci 2024; 65: 38.
16. Liao B, Han Z. Roflumilast reduces myocardial ischemia reperfusion injury in vivo and in vitro by activating the AMPK signaling pathway. Exp Ther Med 2023; 25: 302.
17. Tan Y, Wang X, Gu Y, Bao X, Lu H, Sun X, *et al.* Neutrophil and endothelial cell membranes coassembled roflumilast nanoparticles attenuate myocardial ischemia/reperfusion injury. Nanomedicine (Lond) 2024; 19: 779-797.
18. Li X, Wu H, Peng H, Jiang H. Comparison the effects of finerenone and SGLT2i on cardiovascular and renal outcomes in patients with type 2 diabetes mellitus: A network meta-analysis. Front Endocrinol (Lausanne) 2022; 13: 1078686.
19. Koeche C, Nogueira ACC, Amaral GPDS, Guimarães AJBA, Neiva YB, de Souza AMO, *et al.* Cost-effectiveness of mineralocorticoid receptor antagonists in ischemic and nonischemic heart failure with reduced ejection fraction: Perspective from a universal healthcare system. Value Health Reg Issues 2025; 47: 101084.
20. Marzolla V, Feraco A, Gorini S, Mammi C, Marrese C, Mularoni V, *et al.* The novel non-steroidal MR antagonist finerenone improves metabolic parameters in high-fat diet-fed mice and activates brown adipose tissue via AMPK-ATGL pathway. FASEB J 2020; 34: 1245-1246.
21. Lima Posada I, Soulié M, Stephan Y, Palacios Ramirez R, Bonnard B, Nicol L, *et al.* Nonsteroidal mineralocorticoid receptor antagonist finerenone improves diastolic dysfunction in preclinical non-diabetic chronic kidney disease. J Am Heart Assoc 2024; 13: e032471.
22. Jerome JR, Deliyanti D, Suphapimol V, Kolkhof P, Wilkinson-Berka JL. Finerenone, a non-steroidal mineralocorticoid receptor antagonist, reduces vascular injury and increases regulatory T-cells: Studies in rodents with diabetic and neovascular retinopathy. Int J Mol Sci 2023; 24: 2334.
23. Refaie MMM, Amin EF, Hassan MN, Rifaai RA, Bayoumi AMA, Kamel MY. Sacubitril/valsartan protective effect on induced intestinal ischemia/reperfusion injury via immune modulation of IL6/STAT1 pathway. J Pharm Pharmacol 2024; 76: 788-797.
24. Sanz-Gómez M, Manzano-Lista FJ, Vega-Martín E, González-Moreno D, Alcalá M, Gil-Ortega M, *et al.* Finerenone protects against progression of kidney and cardiovascular damage in a model of type 1 diabetes through modulation of proinflammatory and osteogenic factors. Biomed Pharmacother 2023; 168: 115661.
25. Goyal A, Garabadu D. Roflumilast attenuates cognitive deficits in estrogen insufficient rats. Behav Pharmacol 2020; 31: 671-687.
26. Buege JA, Aust SD. Microsomal lipid peroxidation. Methods Enzymol 1978; 52: 302-310
27. Moron MS, Depierre JW, Mannervik B. Levels of glutathione, glutathione reductase and glutathione S-transferase activities in rat lung and liver. Biochim Biophys Acta 1979; 582: 67-78.
28. Suvarna KS, Layton C, Bancroft JD. Bancroft's theory and practice of histological techniques. 8th ed. London: Elsevier Health Sciences; 2018. p. 73–184.
29. Osho S, Wang T, Horn N, Adeola O. Comparison of goblet cell staining methods in jejunal mucosa of turkey poults. Poult Sci 2017; 96: 556-559.
30. Massoud D, Fouda M, Shaldoum F, Alrashdi BM, AbdRabou MA, Soliman SA, *et al.* Characterization of the small intestine in the southern white-breasted hedgehog (erinaceus concolor) using histological, histochemical, immunohistochemical, and scanning electron microscopic techniques. Microsc Microanal 2023; 29: 2218-2225.
31. Belote BL, Soares I, Sanches AWD, de Souza C, Scott-Delaunay

R, Lahaye L, *et al*. Applying different morphometric intestinal mucosa methods and the correlation with broilers performance under Eimeria challenge. Poult Sci 2023; 102: 102849.
32. KesikV, Guven A, Vurucu S, Tunc T, Uysal B, Gundogdu G, *et al*. Melatonin and 1400 W ameliorate both intestinal and remote organ injury following mesenteric ischemia/reperfusion. J Surg Res 2009; 157: e97-e105.
33. Al-Zahrani MH, Balgoon MJ, El-Sawi NM, Alshubaily FA, Jambi EJ, Khojah SM, *et al*. A biochemical, theoretical and immunohistochemical study comparing the therapeutic efficacy of curcumin and taurine on T-2 toxin induced hepatotoxicity in rats. Front Mol Biosci 2023; 10: 1172403.
34. Zheng Z, Zuo Z, Zhu P, Wang F, Yin H, Peng X, *et al*. A study on the expression of apoptotic molecules related to death receptor and endoplasmic reticulum pathways in the jejunum of AFB1-intoxicated chickens. Oncotarget 2017; 8: 89655.
35. Wang S, Abouzied M, Smith D. Proteins as potential endpoint temperature indicators for ground beef patties. J Food Sci 1996; 61: 5-7.
36. Laemmli UK. Cleavage of structural proteins during the assembly of the head of bacteriophage T4. Nature 1970; 227: 680-685.
37. Towbin H, Staehelin T, Gordon J. Electrophoretic transfer of proteins from polyacrylamide gels to nitrocellulose sheets: Procedure and some applications. Proc Natl Acad Sci 1979; 76: 4350-4354.
38. Harlow E, Lane D. A Laboratory Manual. New York: Cold Spring Harbor Laboratory 1988; 579: 44.
39. Gassmann M, Grenacher B, Rohde B, Vogel J. Quantifying Western blots: Pitfalls of densitometry. Electrophoresis 2009; 30: 1845-1855.
40. Jia Y, Cui R, Wang C, Feng Y, Li Z, Tong Y, *et al*. Metformin protects against intestinal ischemia-reperfusion injury and cell pyroptosis via TXNIP-NLRP3-GSDMD pathway. Redox Biol 2020; 32: 101534.
41. Tang J, Zhuang S. Histone acetylation and DNA methylation in ischemia/reperfusion injury. Clin Sci 2019; 133: 597-609.
42. Marton J, Ciocan RA, Baldea I, Gherman ML, Gheban D, Filip A, *et al*. Molecular mechanisms, dynamic lesions, and therapeutic targets in intestinal ischemia-reperfusion injury: A systematic review. Int J Mol Sci 2026; 27: 1763.
43. Elwany NE, El Salem A, Mostafa Mohamed N, Khalil SS, Mahmoud NM. Rebamipide protects against experimentally induced intestinal ischemia/reperfusion-promoted liver damage: Impact on SIRT1/β-catenin/FOXO1and NFκB signaling. Int Immunopharmacol 119, 110269.
44-Chen K, Xu B, Qiu S, Long L, Zhao Q, Xu J, *et al*. Inhibition of phosphodiesterase 4 attenuates aquaporin 4 expression and astrocyte swelling following cerebral ischemia/reperfusion injury. Glia 2024; 72: 1629-1645.
45. Park EJ, Je J, Dusabimana T, Yun SP, Kim HJ, Kim H, *et al*. Mineralocorticoid receptor antagonism attenuates multiple organ failure after renal ischemia and reperfusion in mice. Int J Mol Sci 2023; 24: 3413.
46. Wang F, Huang H, Wei X, Tan P, Wang Z, Hu Z. Targeting cell death pathways in intestinal ischemia-reperfusion injury: A comprehensive review. Cell Death Discov 2024; 10: 112.
47. Gambaryan S, Mohagaonkar S, Nikolaev VO. Regulation of the renin-angiotensin-aldosterone system by cyclic nucleotides and phosphodiesterases. Front Endocrinol (Lausanne) 2023; 14: 1239492.
48. Lattenist L, Lechner SM, Messaoudi S, Le Mercier A, El Moghrabi S, Prince S, *et al*. Nonsteroidal mineralocorticoid receptor antagonist finerenone protects against acute kidney injury-mediated chronic kidney disease: Role of oxidative stress. Hypertension 2017; 69: 870-878.
49. Özgür BC, Surer H, Yücetürk CN, Karakan T, Özer E, Ogus E. The protective effect of roflumilast and ibuprofen on testicular ischemia reperfusion injury: An experimental study. Ulus Travma Acil Cerrahi Derg 2022; 28: 730-735.
50. Bonato JM, Meyer E, de Mendonça PSB, Milani H, Prickaerts J, Weffort de Oliveira RM. Roflumilast protects against spatial memory impairments and exerts anti-inflammatory effects after transient global cerebral ischemia. Eur J Neurosci 2021; 53: 1171-1188.
51. Short WD, Steen E, Kaul A, Wang X, Olutoye OO, Vangapandu HV, *et al*. IL-10 promotes endothelial progenitor cell infiltration and wound healing via STAT3. FASEB J 2022; 36: e22298.
52. Zhan Y, Deng Q, Jia Y, Chen Z, Zhao X, Ling Y, *et al*. Pdia3 deficiency exacerbates intestinal injury by disrupting goblet and Paneth cell function during ischemia/reperfusion. Cell Signal 2025; 130: 111682.
53. Hassan MI, Ali FE, Shalkami AGS. Role of TLR-4/IL-6/TNF-α, COX-II and eNOS/iNOS pathways in the impact of carvedilol against hepatic ischemia reperfusion injury. Hum Exp Toxicol 2021; 40: 1362-1373.
54. Prionas A, Ziamaoui K, Vanezis K, Reebye V, Habib N, Papalois V, *et al*. Effect of interleukin-10 immunotherapy on renal ischemia-reperfusion injury: A systematic review and meta-analysis of preclinical studies. Int J Mol Sci 2024; 25: 6231.
55. Kırgız Ö, Altuğ ME, Özkan H, Han MC, Akçakavak G, Bozarslan AC, *et al*. 45S5 bioactive glass- ointment positively effects on wound healing in rats by regulating TNFα, Il- 10, VEGF, and TGFβ. J Clin Lab Anal 2024; 38: e25094.
56. Kong J, Cheng W, Chang L, Yu J, Wang R, Xie J. Effects of HMGB1/TLR4 on secretion IL-10 and VEGF in human jaw bone-marrow mesenchymal stem cells. J Appl Oral Sci 2024; 32: e20230304.
57. Feng L, Ren J, Li Y, Yang G, Kang L, Zhang S, *et al*. Resveratrol protects against isoproterenol induced myocardial infarction in rats through VEGF-B/AMPK/eNOS/NO signalling pathway. Free Radic Res 2019; 53: 82-93.
58. Guo HH, Liang JJ, Pan RH, Zheng MF, Qiu YX, Jiang SS, *et al*. Irisin/FNDC5 regulates endothelial function to improve post-stroke-induced cognitive dysfunction by stimulating AMPK-eNOS signaling. Brain Behav 2025; 15: e70767.
59. Engin A. Endothelial dysfunction in obesity and therapeutic targets. Adv Exp Med Biol 2024; 1460: 489-538.